Materials Today Communications xxx (xxxx) xxxx

Contents lists available at ScienceDirect

Materials Today Communications

journal homepage: www.elsevier.com/locate/mtcomm

Antibacterial polymer fibres by rosin compounding and melt-spinning

M. Kanerva[a,*], A. Puolakka[a], T.M. Takala[b], A.M. Elert[c], V. Mylläri[d], I. Jönkkäri[a], E. Sarlin[a], J. Seitsonen[e], J. Ruokolainen[e], P. Saris[b], J. Vuorinen[a]

[a] Tampere University, Materials Science and Environmental Engineering, PO Box 589, FI-33014 Tampere University, Finland
[b] Helsinki University, Department of Microbiology, PO Box 56, FI-00014 University of Helsinki, Finland
[c] Bundesanstalt für Materialforschung und -prüfung (BAM), 12205 Berlin, Germany
[d] Premix Ltd, PO Box 12, FI-05201, Finland
[e] Aalto University, School of Science, Department of Applied Physics, PO Box 15100, FI-00076 Aalto, Finland

ARTICLE INFO

Keywords:
Melt spinning
Fibre
Antibacterial
Thermoplastics

ABSTRACT

The antibacterial features of natural pine/spruce rosin are well established, yet the functionality in various thermoplastics has not been surveyed. This work focuses on the processing of industrial grade purified rosin mixed with polyethylene (PE), polypropylene (PP), polylactic acid (PLA), polyamide (PA) and corn starch based biopolymer (CS). Homopolymer masterbatches were extrusion-compounded and melt-spun to form fibres for a wide range of products, such as filters, reinforcements, clothing and medical textiles. Due to the versatile chemical structure of rosin, it was observed compatible with all the selected polymers. In general, the rosin-blended systems were shear-thinning in a molten condition. The doped fibres spun of PE and PP indicated adequate melt-spinning capability and proper mechanical properties in terms of ultimate strength and Young's modulus. The antibacterial response was found dependent on the selected polymer. Especially PE with a 10 wt% rosin content showed significant antibacterial effects against *Escherichia coli* DH5α and *Staphylococcus aureus* ATCC 12598 when analysed in the Ringer's solution for 24 h.

1. Introduction

The increasing awareness of health hazards and also the pressure to rely on natural raw materials pushes traditional plastic producers to develop functionality using the 'chemistry of nature'. Moreover, the added functionality, such as antimicrobial response, opens up new business strategies for the current polymer industry. Antimicrobial response against several pathogens and, in detail, antibacterial activity in massively produced thermoplastics, such as polyethylene (PE), polypropylene (PP), and polyamide (PA), are typically achieved using silver, oxides of silicon or titanium (SiO_2, TiO_2), antibiotics, or ammonia-based drugs on the product surface or within the polymer structure [1–3]. For example, the rival biocides with an olefin, such as PE, have been compounded and essentially complete kill have been achieved against *Escherichia coli* during a 24 h contact [4]. Likewise, ZnO fillers in polyhydroxyalkanoates have been found to act as biocides in antibacterial biocomposites [5]. The potential health hazards of synthetic additives and requirements for environmental responsibility and ever lower bulk costs have made the industry and research institutions to search for new alternatives [6].

Recently, several polymer compounds have been studied in order to produce fibres and films that are non-toxic, non-allergenic, biodegradable, biocompatible, and would have the required mechanical strength and stiffness for forming textiles or packaging foils [7–9]. For example, chitin and the derived biopolymer chitosan have been found to show antibacterial activity against both Gram-negative (e.g. *E. coli*, *Pseudomonas aeruginosa*) and Gram-positive (e. g. *Staphylococcus aureus*) bacterial strains [10,11]. Hence, chitosan-alginate fibres as well as pure chitosan-chitin nanofibres have been especially developed for medical applications [12,13]. Due to the brittle character of biopolymer films and fibres, composite systems with plasticizers (various glycols) or thermoplastic blends, e.g. including poly(ethylene glycol), poly(vinyl alcohol), poly(acrylic acid), gelatin, starch, or cellulose, are typically studied for practical applications [14]. Most often, it is necessary to modify the surface character and hydrophobicity of nature-derived components to disperse them with thermoplastics, e.g. poly(lactic acid), PLA [15,16]. Multi-composite blends, e.g. those reinforced with natural cellulose derivatives, have been studied to improve the mechanical properties of otherwise weak biopolymers [17]. Entirely natural polymer systems or composites [18], however, are susceptible to fungi and bacterial degradation [19]. When considering natural additives, plant-based oils, such as cinnamon oil, have been reported to have a

* Corresponding author.
E-mail address: Mikko.Kanerva@tuni.fi (M. Kanerva).

https://doi.org/10.1016/j.mtcomm.2019.05.003
Received 2 May 2019; Accepted 6 May 2019

strong antibacterial effect on strains like *S. aureus* and *E. coli* but the mechanical properties decrease when compared to the reference polymers [20]. In contrast, wood rosin, usually extracted of pine or spruce stock, can act as a source of antibacterial activity and also as chemical compatibilizer due to its chemically active structure that is rich in functionality [21–23].

Antibacterial characteristics of direct rosin extracts and rosin acid derivatives have been reported in the current literature. Rosin affects mainly Gram-positive bacteria and the abietic type acids of the rosin compounds have been reported to cause most of the response [24]. Even pure spruce wood particles have an antibacterial effect on *E. coli*, *Streptococcus pneumoniae* and *Salmonella enterica* [25]. It has been found that rosin affects the cell walls of bacteria, such as those of *S. aureus*, hindering the cells' energy synthesis [26]. The source of rosin, polymer additives, and the means of exposure of bacteria onto the rosin containing substance greatly affect the antibacterial response [27]. For packaging applications, rosin-PLA blends have been reported to be successfully antibacterial [28].

The use of rosin in industrially processed materials can face several challenges. First, part of the rosin's chemical components degrade after reaching 200 °C whereas processing temperatures over 220–250 °C are required for extrusion and melt-spinning of PA. Even higher temperatures are needed to process high-performance fibres, such as those from poly(ethylene terephthalate) or not to mention poly(etherether ketone) [29,30]. The primary hypothesis of this work is that rosin-thermoplastic fibres have appropriate antibacterial activity. The secondary hypothesis is that polymers, namely PE, PP, PLA, PA, and corn starch biopolymer, can be compounded into masterbatches with rosin and further processed by using multi-filament melt-spinning. As a starting point, rosin is expected to be compatible with the homopolymers and the main interest is to understand the antibacterial response after fibre processing and the dependence of the antibacterial response on the bacterial contact, i.e., whether the samples are analyzed on agar gel or by continuously purging with an aqueous solution.

2. Experimental

2.1. Selected polymers and rosin

PE and PP granulates of a fibre spinning grade were acquired from Borealis Polymers. PLA (Ingeo), corn-starch polymer (Novamont) and PA (BASF) were acquired as industrial grade. The grades per selected polymer are given in Table 1. Commercial, industrial-grade rosin was provided by Forchem (Finland) and was pine rosin based extract 'gum rosin ww' (batch 16032017, acid value 167 mg KOH/g, softening point 74 °C) in the form of crushed particles.

2.2. Compounding and fibre melt-spinning

The homopolymer masterbatches were extrusion compounded with a model TSE 25 twin-screw extruder (Brabender). The rosin was mixed with polyethylene (PE), polypropylene (PP), polylactic acid (PLA), corn-starch based polymer (CS) and polyamide 6 (PA) with a 10–20% rosin content (per weight). Samples of masterbatches were separated for antibacterial studies and characterisation. The compounding and spinning batches with specific rosin content were formed by mixing pure homopolymer granulates with the rosin-blended masterbatch; the different compounding and spinning series were coded with their polymer abbreviation, letter 'f' for spinning series, and target temperatures (at extruder) during melt-spinning. The different rosin containing compounding and spinning batches are given in Tables 2 and 3 , in addition to the references (i.e. PE, PP, PLA, CS, PA series) that did not contain any rosin. The compounds were melt-spun with a laboratory size melt-spinning machine (Fourné) with a fibre finish and drawing system including four godets and a spool for bobbin. For the spinning, a spinneret nozzle with 10 holes (hole diameter 0.5 mm) was used and, hence, a multifilament, which consists of ten fibres, was obtained. Prior to spinning PLA and PLA based blends, the PLA granulates were dried in an oven (60 °C) for a minimum of 12 h.

Table 1
Acquired polymers for antibacterial fibre spinning trials.

Polymer (abbreviation)	Grade	Provider
Polyethylene (PE)	(HDPE) CG 9620	Borealis polymers
Polypropylene (PP)	HF 420 FB	Borealis polymers
Poly lactic acid (PLA)	2003 D	Ingeo
Corn starch plastic (CS)	Mater Bi	Novamont
Polyamide (PA)	Ultramid B27 E 1	BASF

2.3. Polymer melt characterisation

The rheological behaviour of the compounds was studied using a model MCR 301 rotational rheometer (Anton Paar). A 25 mm-diameter cone-plate measuring system (CP25-4) was applied in a nitrogen atmosphere. Masterbatch granulates were used (rosin content 10–20 wt %) for constant shear rate tests where the shear rate was increased in logarithmic steps from 0.01 to 100 1/s.

2.4. Rosin characterisation

Thermal degradation of rosin was studied using the thermo-gravimetric analysis (TGA) with a TG 209F3 (Netzsch) device by applying a constant heat ramp (10 °C/min) and nitrogen atmosphere. For all the rosin characterisation, solid particles of rosin were directly applied in the as-received form. Subsequently, transition and melting temperatures were determined using differential scanning calorimetry (DSC) by using a model DSC 214 device (Netzsch). Sample (sample weight ≈8–20 mg) pans were sealed by a pierced aluminum lid and the analysis was performed in a nitrogen atmosphere (20–50 ml/min) and by applying a constant heat ramp (10 °C/min).

2.5. Fibre characterisation

2.5.1. Mechanical and physical properties

The effect of rosin compounding on the fibres' stiffness and strength was studied using a tensile testing machine (Testometric, M500) with a 20 N load cell. A gauge length of 10 mm was applied. The tests were carried out at a 20 mm/min displacement rate in a standard environment; at a minimum 10 fibre samples were analysed per spinning batch. Before each mechanical test, the diameter of the fibre was measured using a microscope and used for (engineering) stress calculation. Visual light microscopy (by using DM 2500 M, Leica Microsystems) and scanning electron microscopy (SEM) using a field-emission gun electron microscope (ULTRAplus, Zeiss) were used for studying the fibre surfaces and polished cross-sections. The cross-sectional area, together with the force-strain data, was used to determine Young's modulus for each tested fibre. For moduli, a stress-threshold of 2.0 MPa was used and the strain-range for the linear approximation (fit by Least Squares method) was 0.0016 ± 0.0005, …, 0.021 ± 0.0024 m/m for PE, PP and PLA. For PA and the CS series, a wider range was required due to the scatter of data and to reach a reliable fitting.

2.5.2. Rosin-polymer chemistry

Rosin, the PE homopolymer, fibre samples, and sample fixation epoxy (Epofix, Struers) were characterized using Fourier transform infrared spectroscopy (FTIR) by using a Tensor 27 spectrometer (Bruker). The device was used in Attenuated Total Reflectance (ATR) mode, with a PIKE Technologies GladiATR accessory using a diamond crystal. The measured wavenumber range was 400–4000 cm^{-1}. 128 scans were used for both the background and sample measurements. The atomic force microscope and infrared (AFM-IR) data in this study were

Table 2
Rosin-polymer blend batches for extrusion compounding (series name always refers to the melt-spinning temperature).

Polymer	Rosin content (wt%)	Compounding temperature (°C)	Test series
PE	10, 20	205, 205, 160	PE10-180, PE20-180, PE10-160
PP	10, 20	205, 205, 160	PP10-200, PP20-200, PP10-160
PLA	10, 20	160	PLA10, PLA20
CS	10	130–135	CS10
PA	10	223	PA10

Table 3
Rosin-polymer blend batches for fibre melt-spinning.

Polymer	Rosin content (wt%)	Temperature for spinning (°C)	Test series
PE	10, 20	180, 180, 160	fPE10-180, fPE20-180, fPE10-160
PP	10, 20	200, 200, 160	fPP10-200, fPP20-200, fPP10-160
PLA	10, 20	160–180[a]	fPLA10, fPLA20
CS	10	160	fCS10
PA	10	220[b]	fPA10

[a] Reference homopolymer PLA fibre spun at 190–200 °C.
[b] Reference homopolymer PA fibre spun at 230 °C.

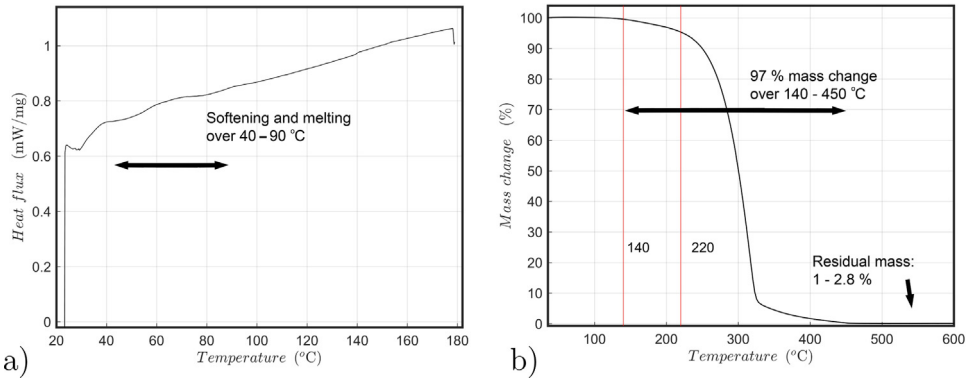

Fig. 1. Thermal analysis of the rosin batch (particles as-received): (a) DSC curve (no background extraction) and; (b) TGA curve for the pure rosin.

obtained by using a NanoIR2S (Bruker/Anasys Instruments), coupled with a multichip QCL source (MIRcat, Daylight Solutions; tunable repetition rate range of 0–500 kHz; spectrum resolution of 0.1 cm^{-1}) covering the range from 900 till 1800 cm^{-1}. An Au-coated silicion probe (contact AFM-IR, cantilever, Anasys Instruments) was employed. The rosin-PE fibre samples for AFM-IR were first embedded in epoxy by casting (Epofix, Struers). After the casting, 100–150 nm thick slices were cut of a pure rosin-PE fibre cross-section by using a cryo-ultramicrotome (Leica Ultracut 7) at −80 to −100 °C. The slices from random locations and depth from a fibre sample were captured on copper grids covered by a carbon film (Electron Microscopy Sciences). The grids with samples were mounted on metallic chips (Ted Pella) for AFM.

2.6. Antibacterial activity

Antimicrobial activity of the polymer samples was tested against indicator bacteria *E. coli* DH5α and *S. aureus* ATCC 12598. The indicators were cultured at 37 °C in lysogeny broth (LB), with 1.5% agar for solid media. Antibacterial tests were performed in both agar media and in Ringer's solution of 1/4 strength (mixture of NaCl, KCl, $CaCl_2$, $NaHCO_3$ and distilled water).

2.6.1. Soft-agar overlay technique

The indicator strains were first cultured overnight in LB broth. 200 µl of the cultures were mixed in 10 ml of melted LB soft-agar (0.75% agar) in a glass tube. Small pieces of granulates and fibres to be tested were put onto a LB agar plate, and the soft-agar containing the indicator bacteria was poured onto the plate. The plates were incubated o/n at 37 °C, after which the possible inhibition zones around the sample pieces were observed.

2.6.2. Antimicrobial activity in liquid

The indicator bacteria were first cultured overnight in LB broth. Colony forming units per ml of the o/n cultures were determined by serial dilutions in 1/4 strength Ringer's solution and plating onto LB agar. From the serial dilutions of 10^2–10^4, 1 ml (about 10^5–10^7 cfu/ml) was used for the antimicrobial tests by mixing with 0.5 g of sample granulates or 0.1 g of fibres in 2-ml Eppendorf tubes. The mixtures were incubated for 24 h at room temperature in a rotator (22 rpm). After incubation, the samples were serially diluted in 1/4 strength Ringer's solution, and plated onto LB agar for determining the bacterial survival by colony counting. All the experiments were performed in triplicates.

3. Results

3.1. Rosin analysis

Rosin DSC and TGA curves are shown in Fig. 1. Based on the DSC, rosin melts after the softening at ≈40 °C following essentially constant behaviour until the liquid phase. The multiple peaks or nonlinearity in the flux curve indicates the natural variation of rosin—the softening point given by the material provider was 74 °C. The variation in the flux over the temperature range of ≈50–100 °C presumably also relates to

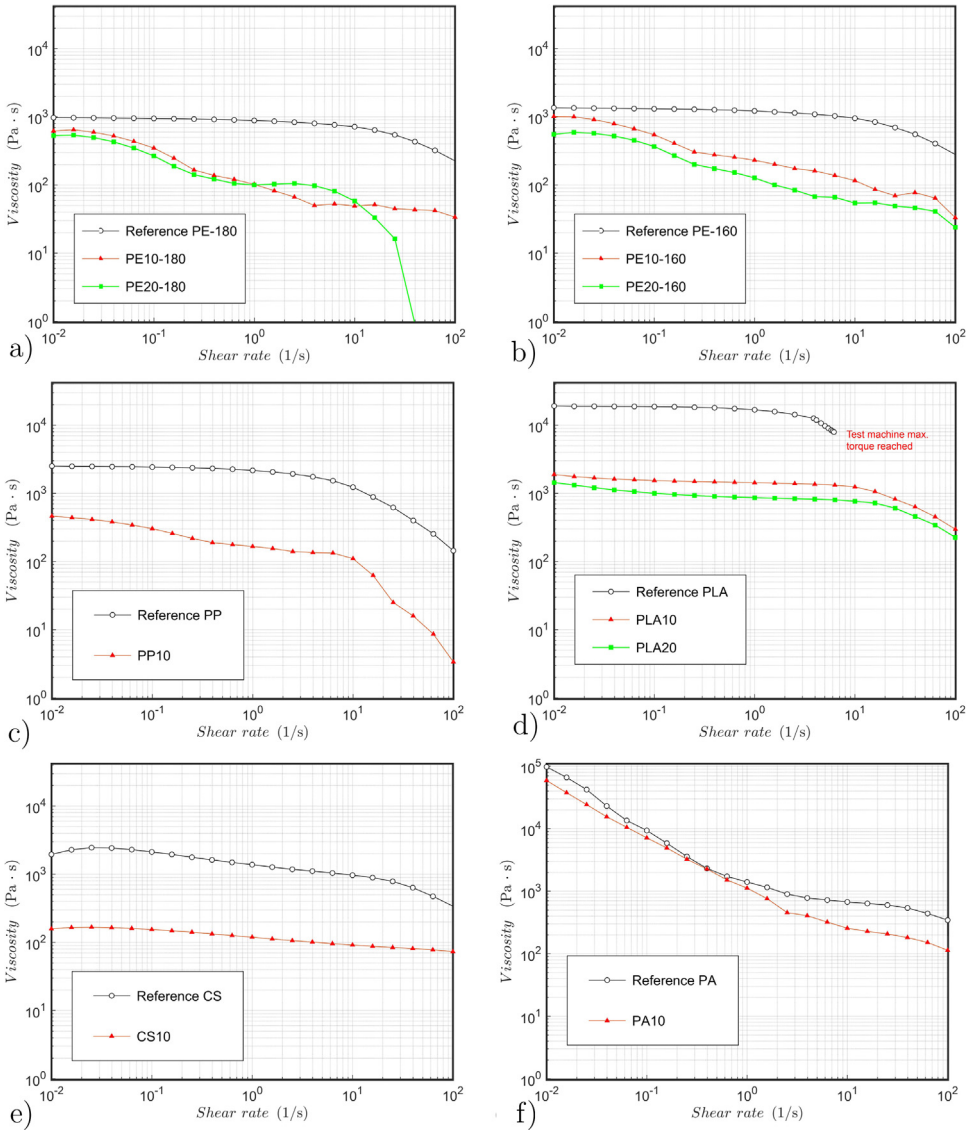

Fig. 2. Viscosity of reference/homopolymers and rosin-blended systems: (a) PE and PE10-180 series measured at 180 °C; (b) PE and PE10-160 series measured at 160 °C; (c) PP and PP10 series measured at 180 °C; (d) PLA and PLA10 series measured at 160 °C; (e) CS and CS10 series measured at 160 °C; (f) PA and PA10 series measured at 180 °C.

the removal of moisture and solvent-type components as well as possible slight crystallinity. The TGA curve (Fig. 1(b)) shows that the final degradation occurs over a temperature range of ≈220–450 °C (onset ≈140 °C), which suggests that rosin in the melt-spinning process of PA fibres (220 °C) might have partly degraded.

3.2. Compound behaviour

Rosin and raw polymer granulates were mixed in the extruder by directly feeding both components into the extruder's hopper. The compounding was carried out at ambient laboratory conditions. The blending of the components was assessed by monitoring the color change of the blend, possible clinging and spitting of rosin either at the hopper or nozzle of the extruder. Rosin was observed to mix readily with thermoplastics and the masterbatches were smooth composites by visual observation with a slight yellowish color. The extruded blend yarn was cut into granulates for further melt-spinning and characterisation.

The behaviour of the blended polymer-rosin systems was studied in terms of the viscosity at different shear rates. The viscosity curves are shown in Fig. 2(a)–(d). The behaviour of different homopolymers was as expected and the changes due to rosin inclusion mostly were established by a significant decrease in viscosity at higher shear rates. Here, all the compounded melts were shear-thinning—yet the viscosity remained essentially constant until a high shear rate level (> 10 1/s) for PE, PP and PLA homopolymers—noting that typical shear rate range during melt-spinning (at nozzle) can reach even 10^3 1/s values. The addition of rosin clearly emphasises the shear-thinning behaviour and, for PLA and CS (Mater Bi polymer), leads to a decade-lower viscosity compared to the homopolymer as a starting point.

Interestingly, the character of PE melt with a rosin content was clearly dependent on the (measurement) temperature. For a higher measurement temperature (180 °C) and higher (20%) rosin content, the viscosity decreased at high shear rates—probably the rosin phase in the compound disintegrates and works as a lubricant. Similar behaviour emerged with PP, measured at 180 °C, but already for a 10% rosin content. This might suggest that the compatibility between rosin and PP is not as good as for PE or the component of lower viscosity (rosin) may act as 'lubricant' and emerge unevenly during the processing at different temperatures. Also, for all the polymer compounds, the viscosity-shear rate dependance seems nonlinear and two plateaus, or shifts, can be distinguished: the first sharp decrease at ≈0.1 1/s and another at

Table 4
Fibre characteristics for homopolymer and rosin-compounded systems.

Series	Mean diameter and deviation (μm)	Mean strength and deviation (MPa)	Logarithmic strain at break (%)
fPE-180	71 ± 7	41 ± 20	308 ± 123
fPE10-180	76 ± 25	19 ± 11	250 ± 118
fPE20-180	100 ± 30	17 ± 7	279 ± 106
fPE-160	53 ± 8	63 ± 17	251 ± 67
fPE10-160	51 ± 7	61 ± 26	279 ± 113
fPP-200	72 ± 11	126 ± 42	263 ± 97
fPP10-200	63 ± 20	95 ± 41	234 ± 102
fPP20-200	71 ± 31	46 ± 23	223 ± 90
fPP-160	47 ± 10	180 ± 73	210 ± 58
fPP10-160	57 ± 9	114 ± 32	216 ± 84
fPLA	55 ± 6	153 ± 47	137 ± 47
fPLA10	84 ± 14	52 ± 15	16 ± 7
fPLA10[a]	116 ± 7	49 ± 5	3 ± 0
fCS	56 ± 5	33 ± 12	177 ± 59
fCS10	59 ± 6	9 ± 4	156 ± 59
fPA	55 ± 7	120 ± 39	233 ± 74
fPA10	52 ± 7	120 ± 40	244 ± 78

[a] Simply melt-spun fibre, not drawn on godets.

≈10 1/s shear rate. It should be noted that polymers may suffer from edge fracture during rotational rheometer measurements at shear rates above the range of 1 to 10 1/s (depending on the polymer and its viscosity) and the measured absolute viscosities therefore appear smaller than they actually are.

3.3. Fibre spinnability and quality

The fibre spinning trials were performed by applying machine parameters (e.g. godet temperatures and speeds) based on experience and initial trials with the rosin-containing blends and a minimum cold-drawing by godets was applied. The fibre characteristics for each successful fibre series are given in Table 4 and stress–strain curves in Figs. 3 and 4 . The first actual trials were run by using the PE and PP masterbatches as well as melt temperatures of 180 °C and 200 °C (at screw), respectively. For the PE and PP mixed with masterbatches with 10% and 20% rosin content, the melt-spinning of fibres was successful, in terms of fibre diameter (63–100 μm) and spinnability (melt draw ratio ≈65). Based on the compounding difficulties in spinning with a 20% rosin content, the PLA, CS and PA series were studied only for a 10% rosin content. The spinning and collection of PLA fibre was challenging as indicated by the significant decrease in viscosity due to rosin blending (see Fig. 2(d)). PLA based fibres lost 66–68% of their strength due to rosin doping, independent of whether the fibre was drawn (on godets) or not. The PLA-rosin fibres were brittle with a negligible ductility (elongation to break ≈6%). Similarly to PLA, the starch polymer based fibres (CS) suffered a significant negative effect due to rosin—in contrast to the PLA fibres, the rosin blending with the CS series plastic led to a very low strength while elongation to break remained essentially unchanged, i.e. the fibre stiffness significantly

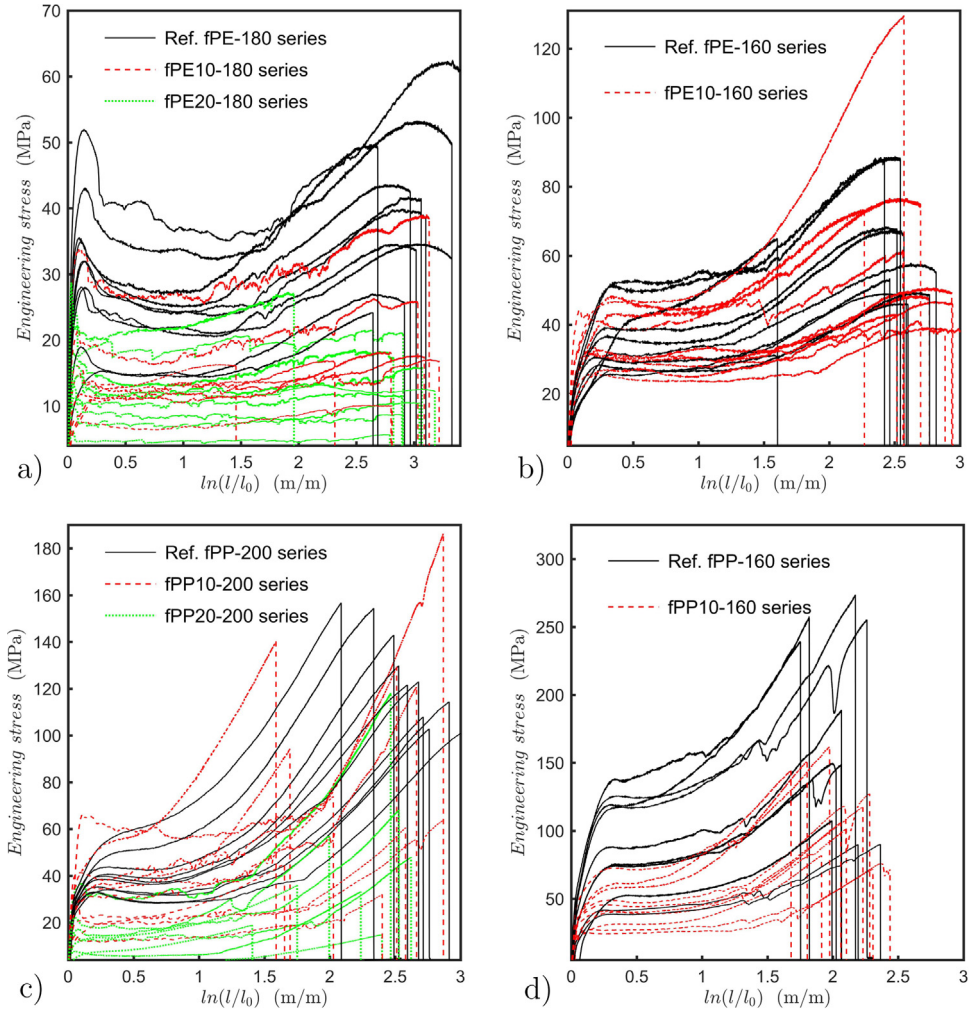

Fig. 3. Stress–strain behaviour of different melt-spun fibres with rosin: (a) fPE-180, fPE10-180 and fPE20-180 series fibres; (b) fPE-160 and fPE10-160 series fibres; (c) fPP-200, fPP10-200 and fPP20-200 series fibres; (d) fPP-160 and fPP10-160 series fibres.

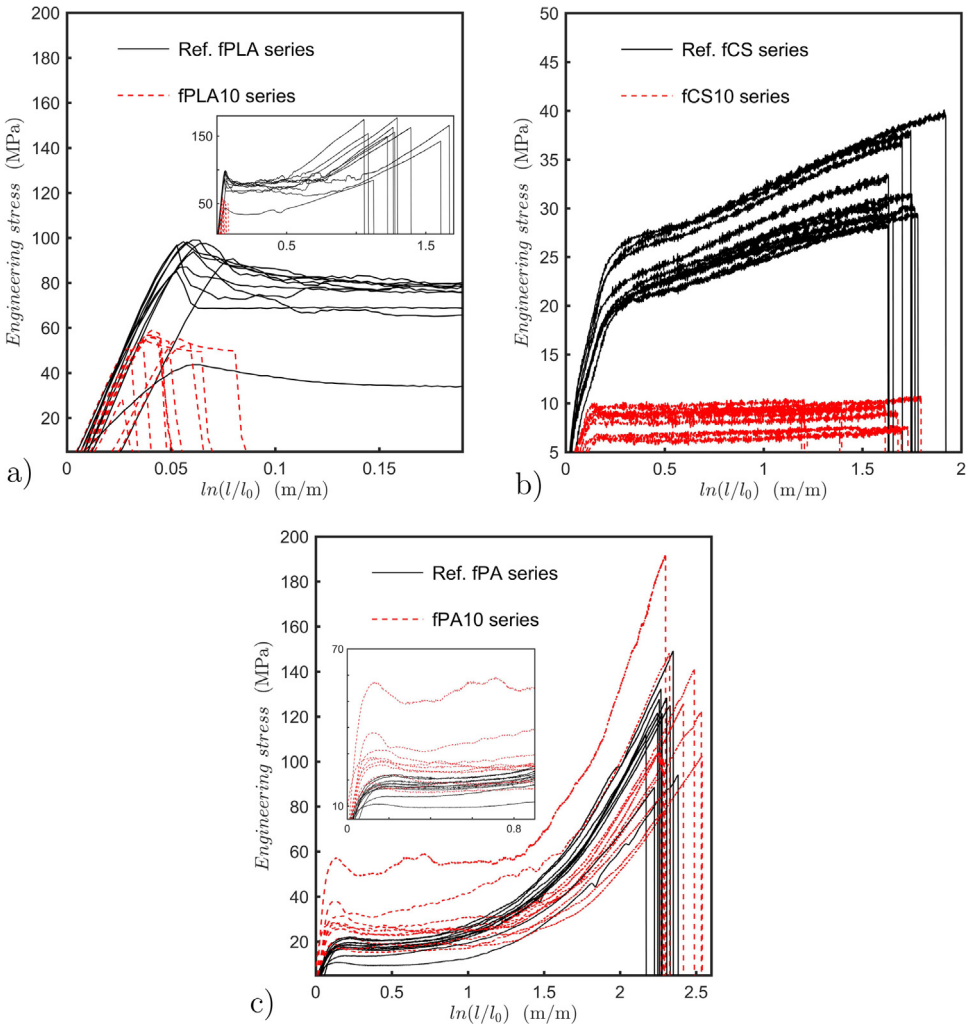

Fig. 4. Stress-strain behaviour of different melt-spun fibres with rosin: (a) fPLA and fPLA10 series fibres; (b) fCS and fCS10 series fibres; (c) fPA and fPA10 series fibres.

Table 5
Fibres' Young's modulus and experimental scatter by coefficient of variation (COV).

Series	Mean modulus and deviation (GPa)	COV (%) over moduli	COV (%) over strength
fPE-180	0.89 ± 0.36	40	49
fPE10-180	0.47 ± 0.33	71	58
fPE20-180	0.73 ± 0.42	57	41
fPE-160	0.53 ± 0.13	25	27
fPE10-160	0.75 ± 0.22	29	43
fPP-200	0.97 ± 0.11	11	33
fPP10-200	0.81 ± 0.35	43	43
fPP20-200	0.40 ± 0.32	79	50
fPP-160	1.23 ± 0.49	40	41
fPP10-160	0.91 ± 0.36	40	28
fPLA	2.07 ± 0.45	22	31
fPLA10	1.80 ± 0.41	23	29
fCS	0.21 ± 0.03	15	36
fCS10	0.07 ± 0.01	15	44
fPA	0.24 ± 0.06	26	33
fPA10	0.48 ± 0.22	44	33

decreased due to rosin in the polymer structure. The PA blends did not suffer any observable strength decrease due to a 10% rosin content compared to the pure homopolymer counterpart.

The stiffness of the spun fibres, in terms of Young's modulus, can indicate good initial compatibility of rosin and the polymer when high values and low scatter of results are reached. The average modulus values and relative deviations for modulus and ultimate strength are given in Table 5. For PE, PP and PLA, the modulus values agree with typical homopolymer moduli and the scatter in the modulus values is clearly lower than in the ultimate strength values—as was expected. Rosin had an effect to decrease the stiffness values and tended to increase the scatter in the modulus values—the effect was stronger the higher the rosin amount. For the PE and PP series, the higher processing temperature led to a lower strength but similar trend for stiffness could not be seen. Presumably, a high processing temperature ruptures the polymer's molecular structure that is reflected to the ultimate behaviour (especially for PP). For PA and the CS series, the modulus values are low and mainly refer to poor quality of the blend where the rosin as well as fibre surface act as voids leading to early yielding and breakage. Based on the mechanical analysis, the spun PE and PP series fibres were the most potential for further analysis (with optimum rosin content ≈10–20%).

3.4. Antibacterial activity

The antimicrobial activity of the melt-spun fibres was determined against both Gram-negative and Gram-positive indicator bacteria *E. coli* and *S. aureus*, respectively. The soft-agar was seeded with the indicators, and overlaid to the plastic samples on agar plate. The rosin-containing fibre samples caused small but rather clear inhibition zone

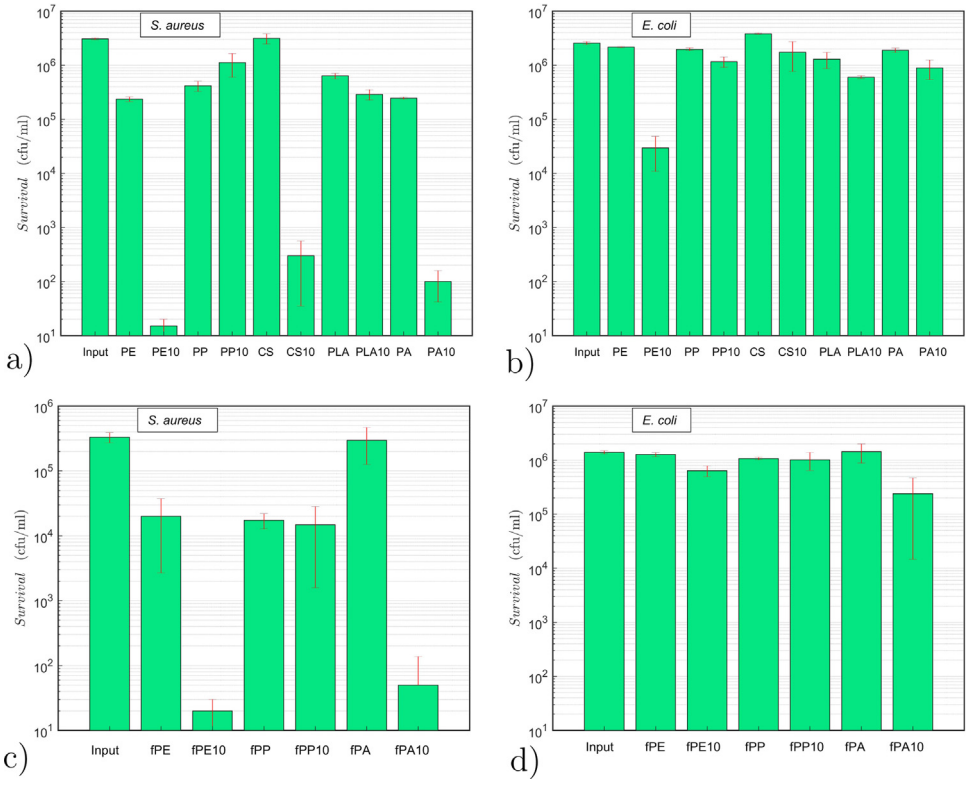

Fig. 5. Antibacterial activity of granulates and fibres in liquid (Ringer's solution, 1/4 strength) after 24 h mixing at room temperature: (a) survival of *S. aureus* (granulates); (b) survival of *E. coli* (granulates); (c) survival of *S. aureus* (fibres); (d) survival of *E. coli* (fibres).

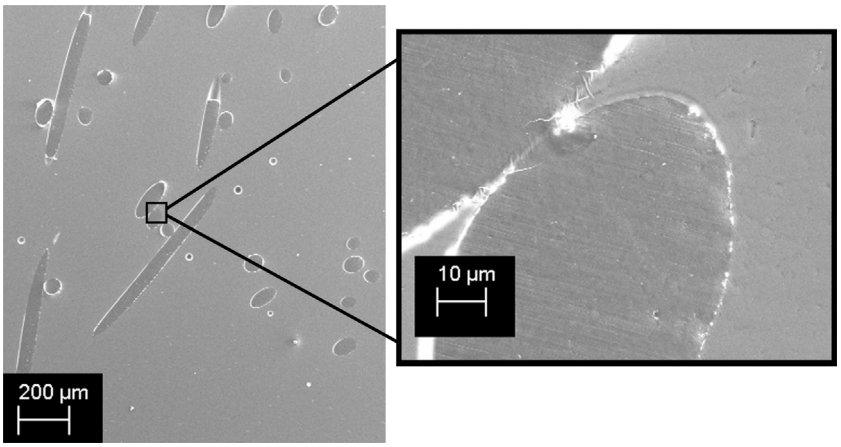

Fig. 6. Cross-section SEM images of PE fibres with rosin (fPE10-160).

with *S. aureus* in soft-agar, but no inhibition could be seen against *E. coli*.

The soft-agar overlay method may not be perfect for studying the fibres and granulates, as the rosin is practically insoluble in water, it does not diffuse well in agar, and thus the bacteria are killed only when in close proximity of the sample. In addition, reliable and comparable data is difficult to obtain from small inhibition zones. Therefore, the antimicrobial activity of the polymeric samples were tested in liquid with rotation, when the thermoplastic and the bacteria are in motion, and the bacteria can get in physical contact with the polymer surface. After rotating 24 h of the sample-bacteria mixture, the survival of the bacteria was determined by plate counting. All the rosin containing granulates except for PP and PLA killed *S. aureus* significantly but the effect was much less with *E. coli*, as shown in Fig. 5. In the fibre form, fPE10 and fPA10 samples were 'effective' against *S. aureus*, whereas PP was clearly less effective. Only PE and PA fibres with a 10% of rosin could inhibit *E. coli* to some extent, but the inhibition was remarkably less than against *S. aureus*.

3.5. Polyethylene-rosin miscibility

The antibacterial results indicated the superiority of PE based fibres against *S. aureus* and *E. coli*. However, it is not well understood how rosin interacts with the molecular network in fibres. SEM imaging shows essentially smooth fibre cross-sections (Fig. 6) and does not indicate any microscopic, separate, rosin phases. Further analysis was carried out for the PE-rosin system via FTIR and nano-IR studies (casting epoxy spectrum given in supplement material). Raw data of the FTIR for epoxy as well as for the presented plots are available for readers [31].

In Fig. 7(a), it can be seen that the addition of rosin leads to absorption of CH_3 stretch and bend related bands (2956, 2867 and

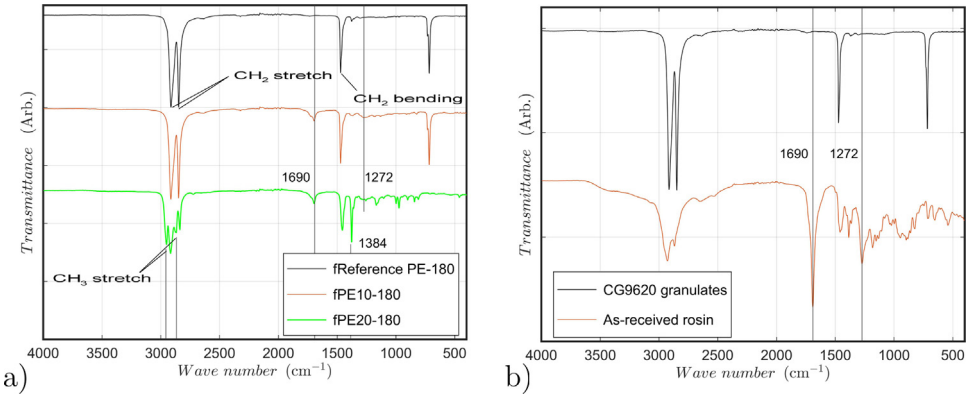

Fig. 7. FTIR spectra of source materials and spun PE and PE-rosin fibres: (a) the effect of rosin content (spinning temperature of 180 °C); (b) as-received PE granulate and rosin spectra.

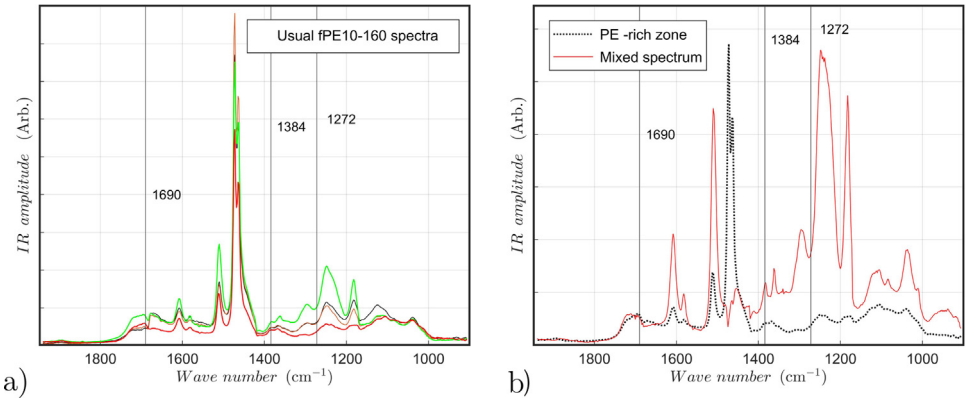

Fig. 8. AFM-IR spectra of PE-rosin fibres: (a) typical random point spectra; (b) comparison with the mixed spectrum of a zone with possible rosin richness.

1384 cm^{-1}, respectively). Based on the pure rosin and pure PE raw material granulates' FTIR spectra (Fig. 7(b)), the appearance of CH_3 related peaks tend to originate from rosin, as well as do the strong absorption at 1690 cm^{-1} and 1272 cm^{-1} from C=O and C–O bond stretch, respectively. Coinciding with the CH_3 absorption bands, the rocking motion related band from multiple CH_2 groups at 715 cm^{-1} is no longer detected in the spectrum (in Fig. 7(a)).

The AFM-IR results are shown for PE-rosin fibre samples in Fig. 8. The rosin is distributed essentially in an even manner. Possible rosin-rich areas ('mixed spectrum') were considered (Fig. 8(b)) yet the spectra do not match those of pure rosin making it unreliable to conclude whether or not local accumulation exists on a sub-nano scale.

4. Discussion

The core of this study is the application of rosin-blended thermoplastic compounds for continuous, melt-spun multifilaments. Therefore, the first task was to analyse the general spinnability in terms of the viscosity of the melts. Since all the selected plastics can be melt-spun below the deterioration temperature of rosin (above 220 °C, Fig. 1), they are applicable as a starting point. However, industrial melt-spinning of fibres requires high enough throughput of properly drawn fibres with properly adjusted balance between strength and elongation (strain to break). In this study, the spun fibres were not drawn to specifically optimised strength–stiffness ratio and, therefore, the strain-hardening behaviour, indicating a good potential to orient and strengthen the polymer, is important. For the homopolymer fibres, basically all the polymers showed strain-hardening behaviour during the tensile tests. For the compounds with rosin (10%), PLA and the corn starch-based biopolymer lost basically all the strain-hardening ability in addition to a dramatic decrease in the fibres' ultimate strength. The degradation of PLA during any high-temperature processing is well-known [32,33] yet the addition of rosin tends to only strengthen this behaviour. Anyhow, various doped PLA compounds can be melt-spun successfully for high take-up velocities when the system is properly controlled in terms of dried source granulates and spinning parameters [34,35]. In contrast to PLA, the PE, PP and PA fibres in this study were characterised by a very high elongation to break and high ultimate strength values with significant strain-hardening—for the homopolymers as well as for the rosin-containing systems. Especially for the PE-rosin spinning at a lower (160 °C) temperature, the rosin addition did not observably decrease the fibre strength and even increased (40%) the initial stiffness (Young's modulus).

In the current literature, PE/PA-rosin systems for industrial fibre production have not been studied. In general, PP is relatively difficult to modify since it is non-polar, hydrophobic and highly crystalline—there are very few attempts to use it for any antibacterial product; cupric oxide doping has been found effective against *E. coli* [36]. In contrast to PP, antibacterial activity in PA and PE fibres has been accomplished with a variety of means [2,4,37]. For other than fibre-form products, e.g. in adhesive applications, good chemical compatibility between PE phases and rosin derivatives (terpenes) has been reported [38,39].

5. Conclusions

This work presents the results of rosin–polymer compounds' viscosity, overall processing effects by temperature and rosin content, fibre performance, and the two-stage analysis of the antibacterial response against indicator bacteria *E. coli* DH5*α* and *S. aureus* ATCC 12598. The compounds involve rosin mixed with polyethylene (PE), polypropylene (PP), polylactic acid (PLA), polyamid (PA) and starch based biopolymer (CS). The fibres made of PE and PP indicated the best mechanical

response in terms of initial stiffness (Young's modulus) and ultimate strength and strain and, thus, the highest potential to be optimized for specific applications. The PLA-rosin fibres reached a high stiffness level but the degradation of the PLA network during processing led to a low ultimate strength and strain. For all the fibre series, the addition of rosin tended to decrease the initial stiffness—PE-rosin fibres indicated the least stiffness degradation and the highest compatibility. Along with the mechanical response, the antibacterial function was found highly dependent on the selected polymer and the type of bacteria as well as the environment of intended (tested) antibacterial effect. PE fibres with a 10 wt% rosin content was verified to show a high antibacterial effect against *S. aureus* ($\approx -100\%$) and a clear effect against *E. coli* (-54%).

Conflict of interest

None.

Acknowledgements

This investigation was funded by a grant from the Business Finland and participating companies (PIHKA, 1763/31/2016). The sample preparation in this study made use of the Aalto University Nanomicroscopy Center (Aalto-NMC) premises. Researchers T. Lehtinen, T. Joki, P. Laurikainen and M. Järventausta are acknowledged for their activities for the work. Borealis is acknowledged for providing raw materials and for supporting raw material shipping/transport.

References

[1] J. Buchéska, Polyamide fibers (PA6) with antibacterial properties, J. Appl. Polym. Sci. 61 (3) (1996) 567–576.
[2] D. Saihi, A. El-Achari, I. Vroman, A. Périchaud, Antibacterial activity of modified polyamide fibers, J. Appl. Polym. Sci. 98 (3) (2005) 997–1000.
[3] M. Pollini, M. Russo, A. Licciulli, A. Sannino, A. Maffezzoli, Characterization of antibacterial silver coated yarns, J. Mater. Sci. Mater. Med. 20 (11) (2009) 2361.
[4] G. Seyfriedsberger, K. Rametsteiner, W. Kern, Polyethylene compounds with antimicrobial surface properties, Eur. Polym. J. 42 (12) (2006) 3383–3389.
[5] A. Díez-Pascual, A. Díez-Vicente, ZnO-reinforced poly(3-hydroxybutyrate-co-3-hydroxyvalerate) bionanocomposites with antimicrobial function for food packaging, ACS Appl. Mater. Interfaces 6 (1) (2014) 9822–9834.
[6] R. Gross, B. Kalra, Biodegradable polymers for the environment, Science 297 (5582) (2002) 803–807.
[7] P.A. Wilbon, F. Chu, C. Tang, Progress in renewable polymers from natural terpenes, terpenoids, and rosin, Macromol. Rapid Commun. 34 (1) (2012) 8–37.
[8] M. Alboofetileh, M. Rezaei, H. Hosseini, M. Abdollahi, Antimicrobial activity of alginate/clay nanocomposite films enriched with essential oils against three common foodborne pathogens, Food Control 36 (1) (2014) 1–7.
[9] A. Ashok, R. Abhijith, C. Rejeesh, Material characterization of starch derived bio degradable plastics and its mechanical property estimation, Mater. Today Proc. 5 (1) (2018) 2163–2170.
[10] Y. Shin, D. Il-Yoo, K. Min, Antimicrobial finishing of polypropylene nonwoven fabric by treatment with chitosan oligomer, J. Appl. Polym. Sci. 74 (12) (1999) 2911–2916.
[11] C. Jarry, C. Chaput, A. Chenite, M.A. Renaud, M. Buschmann, J.C. Leroux, Effects of steam sterilization on thermogelling chitosan-based gels, J. Biomed. Mater. Res. 58 (1) (2002) 127–135.
[12] V.E. Yudin, I.P. Dobrovolskaya, I.M. Neelov, E.N. Dresvyanina, P.V. Popryadukhin, E.M. Ivan'kova, et al., Wet spinning of fibers made of chitosan and chitin nanofibrils, Carbohydr. Polym. 108 (2014) 176–182.
[13] M. Dumont, R. Villet, M. Guirand, A. Montembault, T. Delair, S. Lack, et al., Processing and antibacterial properties of chitosan-coated alginate fibers, Carbohydr. Polym. 190 (2018) 31–42.
[14] A. Toncheva, R. Mincheva, M. Kancheva, N. Manolova, I. Rashkov, P. Dubois, et al., Antibacterial PLA/PEG electrospun fibers: comparative study between grafting and blending PEG, Eur. Polym. J. 75 (2016) 223–233.
[15] X. Huang, X. Qian, J. Li, S. Lou, J. Shen, Starch/rosin complexes for improving the interaction of mineral filler particles with cellulosic fibers, Carbohydr. Polym. 117 (2015) 78–82.
[16] J. Mendes, R. Paschoalin, V. Carmona, A. R Sena Neto, A. Marques, J. Marconcini, et al., Biodegradable polymer blends based on corn starch and thermoplastic chitosan processed by extrusion, Carbohydr. Polym. 137 (2014) 452–458.
[17] H. Nainggolan, S. Gea, E. Bilotti, T. Peijs, S. Hutagalung, Mechanical and thermal properties of bacterial-cellulose-fibre-reinforced Mater-Bi bionanocomposite, Beilstein J. Nanotechnol. 4 (1) (2013) 325–329.
[18] R. Arévalo, T. Peijs, Binderless all-cellulose fibreboard from microfibrillated lignocellulosic natural fibres, Composites Part A 83 (1) (2015) 38–46.
[19] G. de Gonzalo, D. Colpa, M. Habib, M. Fraaije, Bacterial enzymes involved in lignin degradation, J. Biotechnol. 236 (1) (2016) 110–119.
[20] S. Baek, S. Kim, K. Song, Characterization of *Ecklonia cava* alginate films containing cinnamon essential oils, Int. J. Mol. Sci. 19 (1) (2018) 3545.
[21] X. Niu, Y. Liu, Y. Song, J. Han, H. Pan, X. Niu, et al., Rosin modified cellulose nanofiber as a reinforcing and co-antimicrobial agents in polylactic acid /chitosan composite film for food packaging, Carbohydr. Polym. 183 (2018) 102–109.
[22] X. Liu, J. Zhang, rosin. High-performance biobased epoxy derived from, Polym. Int. 59 (2010) 607–609.
[23] Y. Liu, K. Yao, X. Chen, J. Wang, Z. Wang, H. Ploehn, et al., Sustainable thermoplastic elastomers derived from renewable cellulose, rosin and fatty acids, Polym. Chem. 5 (2014) 3170–3181.
[24] T. Söderberg, R. Gref, S. Holm, T. Elmros, G. Hallmans, Antibacterial activity of rosin and resin acids in vitro, Scand. J. Plast. Reconstr. Surg. Hand Surg. 24 (3) (1990) 199–205.
[25] T. Vainio-Kaila, T. Hänninen, A. Kyyhkynen, Effect of volatile organic compounds from *Pinus sylvestris* and *Picea abies* on *Staphylococcus aureus*, *Escherichia coli*, *Streptococcus pneumoniae* and *Salmonella enterica* serovar typhimurium, Holzforschung 71 (2017) 905–912.
[26] A. Sipponen, R. Peltola, J.J. Jokinen, K. Laitinen, J. Lohi, M. Rautio, et al., Effects of Norway spruce (*Picea abies*) resin on cell wall and cell membrane of *Staphylococcus aureus*, Ultrastruct. Pathol. 33 (3) (2009) 128–135.
[27] R. Nirmala, B. Woo-il, R. Navamathavan, D. Kalpana, Y.S. Lee, H.Y. Kim, Influence of antimicrobial additives on the formation of rosin nanofibers via electrospinning, Colloids Surf. B: Biointerfaces 104 (2013) 262–267.
[28] H. Moustafa, N. Kissi, A. Abou-Kandil, M. Abdel-Aziz, A. Dufresne, PLA/PB, bionanocomposites with antimicrobial natural rosin for green packaging, ACS Appl. Mater. Interfaces 9 (1) (2017) 20132.
[29] H. Heuvel, R. Huisman, Effect of winding speed on the physical structure of as-spun poly(ethylene terephthalate) fibers, including orientation-induced crystallization, J. Appl. Polym. Sci. 22 (8) (1978) 2229–2243.
[30] V. Mylläri, T.P. Ruoko, J. Vuorinen, H. Lemmetyinen, Characterization of thermally aged polyetheretherketone fibres – mechanical, thermal, rheological and chemical property changes, Polym. Degrad. Stab. 120 (2015) 419–426.
[31] M. Kanerva, T.M. Takala, A.M. Elert, V. Mylläri, I. Jönkkäri, E. Sarlin, J. Seitsonen, J. Ruokolainen, P. Saris, J. Vuorinen. Data for: Antibacterial thermoplastic fibres by rosin compounding and melt-spinning. Mendeley data, doi:10.17632/5zy62mmr8w.1.
[32] M. Williamson, A. Coombes, Gravity spinning of polycaprolactone fibres for applications in tissue engineering, Biomaterials 25 (3) (2004) 459–465.
[33] B. Eling, S. Gogolewski, A. Pennings, Biodegradable materials of poly(l-lactic acid): 1. Melt-spun and solution-spun fibres, Polymer 23 (11) (1982) 1587–1593.
[34] P. Pötschke, T. Andres, T. Villmow, S. Pegel, H. Brünig, K. Kobashi, et al., Liquid sensing properties of fibres prepared by melt spinning from poly (lactic acid) containing multi-walled carbon nanotubes, Compos. Sci. Technol. 70 (2) (2010) 343–349.
[35] G. Schmack, B. Tändler, G. Optiz, R. Vogel, H. Komber, L. Häussler, et al., High-speed melt spinning of various grades of polylactides, J. Appl. Polym. Sci. 91 (2) (2004) 800–806.
[36] S. Kara, M. Ureyen, U. Erdogan, Structural and antibacterial properties of PP/CuO composite filaments having different cross sectional shapes, Int. Polym. Proc. 31 (4) (2016) 398–409.
[37] B. Kutlu, P. Schröttner, A. Leuteritz, R. Boldt, E. Jacobs, G. Heinrich, Preparation of melt-spun antimicrobially modified LDH/polyolefin nanocomposite fibers, Mater. Sci. Eng. C 41 (2014) 8–16.
[38] L. Svenningsen, D. Strelow, M. Alper, M. Hoppa-Willbrandt, Antimicrobial hot melt adhesive, US Patent 6,664,309 B2, 2003.
[39] M. Barrueso-Martínez, T. del Pilar Ferrándiz-Gómez, M. Romero-Sánchez, J. Martín-Martínez, Characterization of EVA-based adhesives containing different amounts of rosin ester or polyterpene tackifier, J. Adhesion 79 (8-9) (2003) 805–824.